CYCLABILITY OF THE LITHIUM ELECTRODE

M. GARREAU

Physique des Liquides et Electrochimie, Université Pierre et Marie Curie, Tour 22 - 4, Place Jussieu, 75230 Paris Cédex 05 (France)

Summary

The cyclability of lithium in aprotic media at ambient temperature is discussed in terms of the properties of passivating films that are formed at the electrode surface by the reaction of the metal with the various electrolytes. Some models and experimental techniques are examined with the object of establishing guidelines in the search for successful operational systems and/or optimal cycling conditions.

Introduction

Over the last twenty-five years, lithium has been intensively studied throughout the world as being the best negative electrode candidate capable of meeting the increasing demand for high specific-power and high specific-energy batteries.

The major problem encountered when developing high performance lithium batteries arises from the particularly strong reducing potential of the metal: lithium is thermodynamically unstable in the solvents used to prepare the electrolytes. However, in some cases the unavoidable chemical attack can lead to the formation of surface layers that provide the electrode surface with a kinetic stability sufficient to avoid an excessive consumption of lithium during long storage periods. As an example, one may quote the results obtained by the SAFT Laboratories using a mixture of tetrahydrofuran and dimethoxyethane: 96% of the capacity was recovered after a fifteen-year storage period. Nevertheless, the capability of preventing, to varying degrees, the chemical corrosion of the lithium electrode under storage conditions is not the only requirement of the surface layers. They must also have a sufficient conductivity for the Li^+ ions and possess suitable mechanical properties in order to maintain their protective capabilities despite volume changes associated with the anodic dissolution and cathodic deposition of lithium.

Many reports on the surface (or passivating) layers, together with tentative explanations of the mechanism by which these layers function, have been published during the last two decades and have been regularly reviewed

0378-7753/87/$3.50

[1 - 4]. Most of these data are difficult to exploit as they are fragmentary and only apply to experimental conditions that are scarcely comparable. Therefore, rather than present an analysis of reported studies, which would necessarily be disputable and incomplete, this paper simply illustrates the efforts made in a number of directions — modelling and experimental techniques — with the aim of developing guide-lines in the search for successful operational systems and/or optimal cycling conditions.

Models of passivating layers

The solid electrolyte interphase (SEI) model

The main hypothesis on which this model [4] is built supposes that the passivating layer is instantly formed when the lithium is brought into contact with the electrolyte, so that there is never prolonged direct contact between the electrode and the solution. These layers consist of mineral compounds, and the ionic migration of the Li^+ ions through the protective film which acts as a Solid Electrolyte Interphase (SEI) is the rate-determining step of the electrode kinetics. The main characteristics of the layer associated with this model are generally:

(i) a high reaction resistance (at least 100 Ω cm^2);
(ii) a low interfacial capacitance (a few μF cm^{-2});
(iii) a Tafel slope of at least hundreds of millivolts.

The polymer electrolyte interphase (PEI) model

The passivating layers formed in some organic electrolytes containing low quantities of residual water do not behave as solid electrolyte interphases. The behavior observed is more satisfactorily described in terms of an interphase comprising a porous polymeric membrane whose pores are filled with the electrolyte [5 - 7]. In the corresponding model — the so-called Polymer Electrolyte Interphase (PEI) model — the electrode surface is not uniformly accessible, *i.e.*, opposite to that which occurs in the SEI model. As shown in Fig. 1(a), the lithium surface is divided into two parts: an inactive part of relative area *0* isolated from the electrolyte by the solid portion of the membrane, and an active part — the botton of the pores — of relative

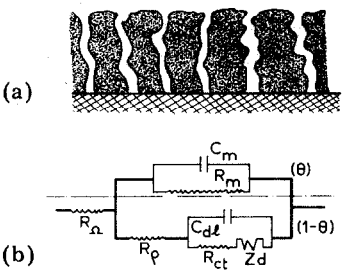

Fig. 1. PEI model. (a) Schematic view of the porous structure; (b) equivalent electrical circuit.

area $(1-\theta)$. It is then assumed that the electrode behaviour of the active area is governed by the charge-transfer process — as generally accepted by a number of experts in the field [1, 2, 8, 9] — and controlled to some extent by the diffusion process of the Li^+ ions inside the electrolyte-filled pores (matrix electrolyte). This model is compatible with reaction resistance and Tafel slopes lower than those associated with the SEI model.

The PEI model describes a limiting situation in which the interphase at the bottom of the pores does not significantly impede the charge-transfer reaction. Such a situation occurs when the pores are sufficiently narrow to allow the capillary forces to strongly modify the physicochemical properties inside these pores, and to provide the lithium surface with a medium that is less agressive than the bulk of the electrolyte but less structured than the solid electrolyte interphase. In some cases, the actual situation is certainly an intermediate one in which the Li^+ ions must migrate and diffuse successively through an SEI and the electrolyte-filled pores of the passivating layer. The situation is then relevant to both the PEI and SEI models.

Experimental techniques

Galvanostatic measurements

Plots of voltage as a function of time, *i.e.*, $V = V(t)$, under galvanostatic conditions have been intensively used since study began on the cycling process of the lithium electrode. An obvious criterion for ideal behaviour of a passivating layer is zero variation in the voltage during the charging and discharging periods of a cycle, and no change in the $V = V(t)$ curve during the continutation of the cycling process. For example, one may cite the cycling of lithium in an $LiClO_4$ (1 M)/propylene carbonate (PC) electrolyte with quite low current and charge densities ($j = 1$ mA cm^{-2}; $Q = 1$ C cm^{-2}). The voltage recorded during the first cycle is sufficiently stable to give a satisfactory performance of this electrode in a rechargeable battery: the $V = V(t)$ curve does not vary significantly in the course of consecutive cycles. Such results strongly indicate the possibility of long cycle lives. Indeed, more than 500 cycles were achieved [10] without any significant deterioration of

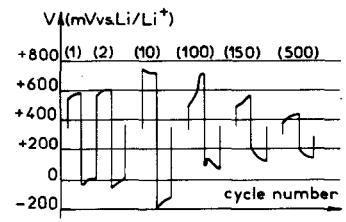

Fig. 2. Cycling behaviour of a lithium–aluminium electrode in PC/$LiClO_4$ (1 M). $Q = 2.5$ C cm^{-2}; $j = 2$ mA cm^{-2}.

the electrochemical properties of the electrode. By contrast, the use of current or charge densities incompatible with long life performance generally gives rise to rapid changes in the initial $V = V(t)$ curves. However, this criterion, although helpful, is far from being absolute. Figure 2 shows a case when an initial increase in both the dissolution and deposition voltages did not lead to rapid failure on cycling. By contrast, the system exhibited a noticeable improvement in its kinetics; this departure from the expected behaviour was probably due to an increase in the actual active surface of the aluminium–lithium electrode [11, 12]. On the other hand, there have been instances when cycling failure appears suddenly without any warning.

Potentiostatic measurements

The electrode surface can be locally submitted to uncontrolled high overpotentials (η), under galvanostatic conditions, especially at the very beginning of experiments when the lithium surface is covered with a heterogeneous and highly resistive passivating layer. These high overpotentials can lead to undesirable electrochemical side-reactions that can irreversibly render the electrode unsuitable for cycling. To prevent this situation developing, experiments can be conducted under potentiostatic conditions, that is by imposing a constant value, not on an overall — and arguable — property of the cell (j), but on a particular property (η).

Potentiostatic dissolutions have been regularly performed in our laboratory to eliminate passivating layers formed during the preparation of electrode surfaces in a glove box. For example, with $LiClO_4$/PC electrolytes, two types of current–time curves, $j = j(t)$, have been obtained. The first was observed when the overpotential was higher than 200 mV. A high current density was first obtained, then the current decreased and a steady state was reached. Inspection of the electrode revealed a waxy, transparent layer that could not be removed by any further electrochemical treatment. A second type of behaviour was observed at overpotentials below 200 mV. The current density was increased continuously and reached a stationary value when the amount of electricity supplied to the cell exceeded 10 C cm^{-2}; this led to a lithium surface with a clearly defined polycrystalline structure. The latter procedure was used to prepare reproducible "clean" surfaces. Scanning electron microscopy (SEM) studies confirmed the cleaning effect of anodic dissolution carried out at these low overpotentials and showed the necessity to plate lithium on such surfaces to avoid any dendrite formation, even at a charge density as low as 1 C cm^{-2}.

Studies of the development of the current density during cycling operations performed under potentiostatic conditions allow rapid estimation of the influence of the charge density on the rate of deterioration of the passivating layer properties, and thereby the probability of achieving long cycle life. For example, the curves shown in Fig. 3 rule out the use of high charge densities for long-life batteries with the system under study.

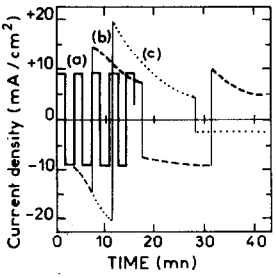

Fig. 3. Current density under potentiostatic control. Overpotential: η = 50 mV. Charge densities: (a) 1 C cm^{-2}; (b) 5 C cm^{-2}; (c) 10 C cm^{-2}.

Electrode impedance spectroscopy

Electrode impedance spectroscopy is generally more convenient than galvanostatic or potentiostatic techniques for separating the different processes involved in electrode kinetics. These processes can be described by specific equivalent circuits associated with each passivating-layer model.

(i) SEI model

Assuming that the rate-determining step of the electrode process is the migration of the Li^+ ions through the SEI, the basic equation for ionic conduction in solids leads, for high field conditions, to the following relation:

$$i = i_o \exp(b/L)\eta \quad (1)$$

where i_o and b are constants characteristic of the nature of the layer, L is the thickness of the layer, and η is the overpotential.

Equation (1) leads to "Tafel" slopes estimated by Peled [4] as being of the order of 400 mV. Some experimental measurements reported by this author [4] are, in fact, even higher, *e.g.*, 0.45 - 3.15 V in PC solution; ~2 V in thionyl chloride solutions.

For low field conditions, the current is governed by Ohm's Law which was used to determine resistivity values for some SEIs ($10^7 \rightarrow 10^{10}$ Ω cm) [4].

When the rate-determining step of the electrode process is the migration of Li^+ inside the SEI, the equivalent circuit is a capacitor (C_{SEI}) in parallel with an ionic resistor (R_{SEI}), Fig. 1(b). The capacitance of the SEI is given by the parallel-plate-capacitor equation:

$$C_{SEI} = \frac{\epsilon A}{3.6\pi L \times 10^{12}} \quad (2)$$

where L and ϵ are, respectively, the thickness and the dielectric constant of the SEI, and A is the electrode area. Equation (2) leads to thicknesses in the range 25 - 200 A [4]. A number of examples of systems relevant to this description are given in ref. 4. The semi-circle (a) in Fig. 4 illustrates a typical SEI impedance spectrum plotted in the complex plane (high reaction resistance ($R \sim 350\ \Omega\ cm^2$), low interfacial capacitance ($C \sim 0.5\ \mu F\ cm^2$)).

This curve corresponds to a lithium electrode immersed in an $LiClO_4$ (1 M)–PC electrolyte, before submitting it to an anodic cleaning treatment, the electrode having been exposed for a long time in a contaminating atmosphere. In this case the layer can act as the SEI component.

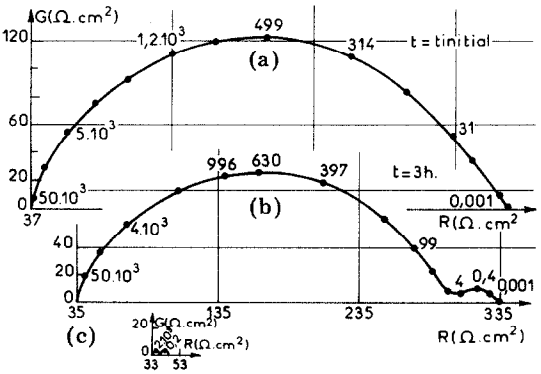

Fig. 4. Impedance spectrum at rest potential of a lithium electrode — not submitted to an initial anodic "cleaning" — stored in PC/$LiClO_4$ (1 M) electrolyte: (a) 0 h; (b) 3 h; (c) 18 h. Frequency in Hz.

(ii) PEI model

The basic equations representing an electrochemical process controlled both by an ionic diffusion of the Li^+ ion through electrolyte-filled pores and the charge transfer reaction at the lithium surface, are as follows [5]:

$$i = i_o \left\{ \frac{C}{C_o} \exp \frac{\alpha F \eta}{RT} - \exp \frac{(\alpha - 1) F \eta}{RT} \right\} \quad (i.e., \text{Butler–Volmer equation}) \quad (3)$$

$$i = \frac{2DF(C - C_o)}{d} \quad (i.e., \text{Fick's law; Nernst's model}) \quad (4)$$

where C and C_o are, respectively, the ion concentrations on the lithium surface and in the bulk of the electrolyte, D is the diffusion coefficient of the Li^+ ion along the length d of the pores, and i_o is the exchange current density. The diffusion impedance Z_d is given by the Drossbach–Schultz equation [13]:

$$Z_d = R_d \frac{\tanh \sqrt{j2\pi f d^2/D}}{\sqrt{j2\pi f d^2/D}} \quad (5)$$

where the specific diffusion resistance R_d, at equilibrium is given by the relation:

$$R_d = \frac{RTd}{2C_o F^2 D} \quad (6)$$

The imaginary component reaches a maximum for the Drossbach–Schultz frequency f^* defined by

$$2\pi f^* \sim 0.4D/d \quad (7)$$

Equations (6) and (7) lead to the following relations:

$$d = \frac{0.2RT}{2\pi f^* C_o F^2 R_d} \quad (8)$$

and

$$D = \frac{0.1R^2T^2}{2\pi f^* C_o^2 F^4 R_d^2} \quad (9)$$

which enable estimation of the values of the d and D parameters of the passivating layer.

The equivalent circuit for the PEI model is given in Fig. 1(b). Over the inactive area, θ, of the electrode surface, the circuit consists of the capacitance C_m and bulk resistance R_m of the solid portion of the membrane. Over the active area $(1 - \theta)$, the circuit is represented by the electrolyte resistance (R_p) inside the pores, the double-layer capacitance (C_{dl}), the charge transfer resistance (R_{ct}) and the diffusion impedance (Z_d). When R_{ct} and R_d are of similar magnitudes, the impedance diagram plotted in the complex plane consists of two distinct parts: (i) a high frequency semi-circle (between 10^5 and a few Hz) that is characteristic of the charge transfer process; (ii) a low frequency loop (between a few Hz and 10^{-3} Hz) that is associated with the diffusion process.

Results and discussion

There are several examples of passivating layers for which the diffusion of Li^+ ions appears to be a secondary limiting factor. This applies when the lithium electrode is submitted to anodic overpotentials corresponding to cleaning conditions. The resulting values of R_{ct} are in good agreement with those expected from the derivation of eqn. (3). These values are (within the accuracy of the measurements) equal to the polarization resistances deduced from the stationary polarization curve [14], and are correctly related to Li^+ concentrations. The Tafel slope deduced from the polarization curve is near the 120 mV expected from eqn. (3) [11].

With the same system, the ion diffusion through the passivation layer becomes important when the electrodes are not used under cleaning conditions ($\eta < 25$ mV), or are studied during storage periods. The analysis of the impedance diagrams obtained at the initial time of storage for various Li^+ concentrations leads to d values that exhibit little variation with concentration ($d \sim 2.1 \times 10^{-5}$ cm). This observation demonstrates that the structure of the initial passivating layer is determined not by the concentration of the solute, but rather by the nature of the solvent. However, the characteristics of the layers show marked changes during storage of electrodes. For example, after 18 h D increased from approximately 5×10^{-10} cm^2 s^{-1} to about 10^{-8} cm^2 s^{-1}, and d increased to approximately 10^{-3} cm (a value close to that obtained from SEM measurements). This behaviour is probably due to the progressive insertion inside the pores of lithium carbonate micro-crystals whose presence was previously identified by electron microscopy studies [10].

The type of structure (SEI or PEI) of the passivating layer observed when immersing a lithium surface in an electrolyte must not be considered

as necessarily immutable. For example, Fig. 4 shows the impedance characteristics obtained with a PC/$LiClO_4$ (1 M) electrolyte after: (a) immersion of the electrode; (b) 3 h storage; (c) 18 h storage. Curve (a) corresponds to SEI behaviour, and curves (b) and (c) to PEI behaviour.

Analysis of impedance diagrams can also yield useful information on the reversible or inhibiting aspects of storage or cycling procedures. For example, studies of an $LiClO_4$ (1 M)/dioxolane electrolyte (Fig. 5) show the restoration of an initial passivating layer by anodic stripping. By contrast, such a tentative complete restoration failed when using an $LiClO_4$/PC electrolyte: the diffusion process persisted in spite of the anodic stripping, and satisfactory cycling conditions could not be obtained.

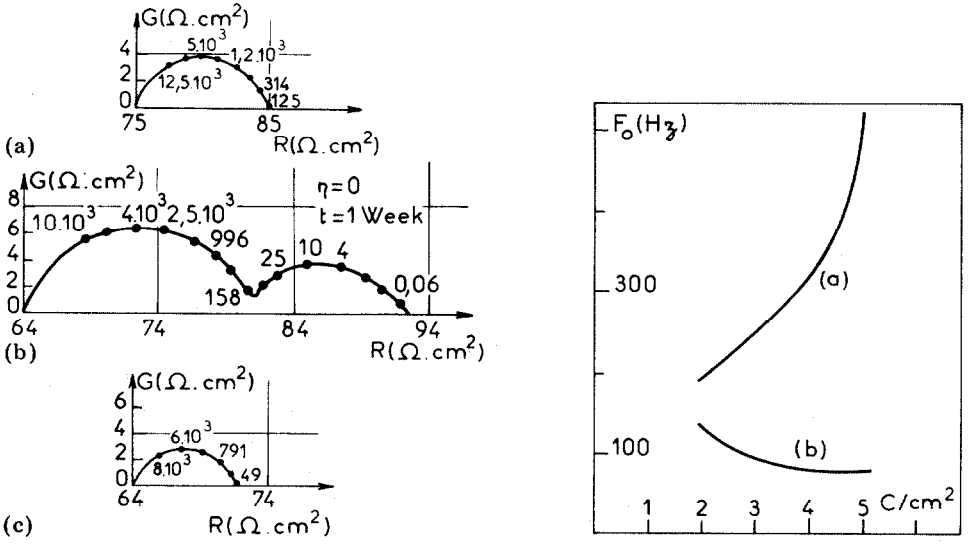

Fig. 5. Restoration of the initial properties of a passivating layer formed in an $LiClO_4$ (1 M)/dioxolane electrolyte. (a) 0 h; (b) after 18 h storage in electrolyte; (c) after anodic "cleaning" treatment.

Fig. 6. Frequency, F_0, corresponding to the maximum of the high-frequency semi-circle part of the impedance spectrum as a function of charge density, Q. (a) End of discharge; (b) end of charge. Electrolyte: sulfolane/$LiAsF_6$, at 30 °C.

Recently, exploratory efforts have been made to follow, *in situ*, changes in the characteristics of passivating layers during cycling processes. Figure 6 shows the behaviour of an intensive parameter of the impedance diagram, namely, the frequency, F_0, corresponding to the maximum of the high freqency semi-circle, as a function of the charge density, Q. Curve (a) corresponds to the end-of-discharge, and curve (b) to the end-of-charge. The difference in F_0 between curves (a) and (b) does not vary linearly with Q, but increases sharply as electrode failure is approached. It should be noted that the corresponding $V = V(t)$ curve did not give any warning of electrode failure.

Conclusions

The techniques and models illustrated above serve to improve the understanding of the mode of action of passivating layers on lithium, and to define efficient and rapid tests required in the search for systems with better performance. However, to date, not one of these techniques appears to be a universal panacea; more precise data must still be accumulated, analysed and discussed in terms of basic models, such as the SEI and PEI types, or in terms of more elaborate models that incorporate contributions to the conduction process of the materials, *i.e.*, polymer electrolytes which constitute the walls of the pores [15, 16].

References

1 J. O. Besenhard and G. Eichinger, *J. Electroanal. Chem., 68* (1976) 1; *72* (1976) 1.
2 A. N. Dey, *Thin Solid Films, 43* (1977) 131.
3 V. R. Koch, *J. Power Sources, 6* (1981) 357.
4 E. Peled, in J. P. Gabano (ed.), *Lithium Batteries*, Academic Press, London, 1983, Ch. 3.
5 J. Thevenin, *J. Power Sources, 14* (1985) 45.
6 M. Froment, M. Garreau, J. Thevenin and D. Warin, *J. Microsc. Spect. Electron., 4* (1979) 111.
7 G. Nazri and R. H. Muller, *J. Electrochem. Soc., 132* (1985) 2050.
8 R. Jasinski, *High Energy Batteries*, Plenum Press, New York, 1967.
9 J. Jorne and C. W. Tobias, *J. Electrochem. Soc., 121* (1974) 994.
10 M. Garreau, J. Thevenin and D. Warin, *Prog. Batteries Solar Cells, 2* (1979) 54.
11 M. Garreau, J. Thevenin, D. Warin and Ph. Campion, *Proc. Int. Workshop on Lithium Batteries Electrochemistry*, The Electrochem. Soc., Softbound Series, Pennington, NJ, 1980, p. 158.
12 M. Garreau, J. Thevenin and M. Fekir, *J. Power Sources, 9* (1983) 235.
13 P. Drossbach and J. Schultz, *Electrochim. Acta, 9* (1964) 1391.
14 I. Epelboin, M. Garreau and J. Thevenin, *Electrochem. Soc., 124* (1977) 1030.
15 P. R. Sørensen, *Electrochim. Acta, 27* (1982) 1671.
16 M. Keddam, C. Rakotomavo and H. Takenouti, *J. Appl. Electrochem., 14* (1984) 437.